Biosensors and Bioelectronics 61 (2014) 541–546

Contents lists available at ScienceDirect

Biosensors and Bioelectronics

journal homepage: www.elsevier.com/locate/bios

In-situ DNA hybridization detection with a reflective microfiber grating biosensor

Dandan Sun, Tuan Guo, Yang Ran, Yunyun Huang, Bai-Ou Guan *

Institute of Photonics Technology, Jinan University, Guangzhou 510632, China

ARTICLE INFO

Article history:
Received 4 April 2014
Received in revised form
24 May 2014
Accepted 29 May 2014
Available online 9 June 2014

Keywords:
Microfiber grating
Optical fiber
Optical biosensor
DNA hybridization detection

ABSTRACT

A label-free fiber-optic biosensor with a reflective microfiber Bragg grating (mFBG) configuration for *in-situ* DNA hybridization detection has been proposed and experimentally demonstrated. A single straight Bragg grating inscribed in the silica microfiber provides two well-defined resonances in reflection, which show different response to external medium refractive index (RI) and present the same temperature sensitivity. By monitoring the wavelength separation between these two resonances, temperature-compensated RI measurement has been achieved. The label-free bio-recognition scheme used demonstrates that the sensor relies on the surface functionalization of a monolayer of poly-L-lysine (PLL), synthetic DNA sequences that bind with high specificity to a given target. In addition to monitoring the surface functionalization of the fiber in real-time, the results also show how the fiber biosensor can detect the presence of the DNA hybridization with high specificity, in various concentration of target DNA solutions, with lowest detectable concentration of 0.5 μM.

1. Introduction

In-situ detection of DNA hybridization has attracted great attention because the analysis of specific DNA sequences is an important method in health and epidemic prevention, disease diagnosis, drug research, environmental science and biological engineering (Fan et al., 2008; Nguyen et al., 2012; Candiani et al., 2013). Fiber optic sensors have been implemented for label-free DNA detection in the recent years because of intrinsic biocompatibility for real-time biochemical measurement with high sensitivity and good reliability (Wang et al., 2006; Chen et al., 2007; Delport et al., 2012; Yin et al., 2013). As a promising photonic device, fiber Bragg grating (FBG) provides advantages of wavelength encoding (multiplex ability), reflective measurement (compact size), excellent wavelength response (high sensitivity), and good reproducibility (well-established fiber grating fabrication technique), make it a good candidate as biosensor. Existing works of fiber grating biosensors are mainly using long period grating (LPG) or tilted FBG (TFBG), in which strong evanescent cladding modes can be achieved for surrounding refractive index (RI) measurement without fiber tapering or etching process (Tripathi et al., 2012; Guo et al., 2014; Voisin et al., 2014). However, straight FBGs inscribed in standard single mode fibers (SMFs) work on fundamental core modes which are inherently insensitive to events outside the fiber cladding, thus they cannot be directly used for RI measurement. Since 2003, Tong et al. reported their work of drawing a standard fiber down to sub-wavelength scale (Tong et al., 2003). This new concept of "microfiber" opens up new sensing modalities arising from two contributions: it extremely decreases the sensor device in size (range from a few micrometers to tens of nanometers in diameter) with low transmission attenuation, and more importantly, it provides strong evanescent fields out of fiber cladding for high-sensitive biochemical measurement (i.e. cells, molecule and DNA) (Leung et al., 2007, 2008; Long et al., 2008; Corres et al., 2008; Zibaiia et al., 2010; Tian et al., 2011; Latifi et al., 2012; Li et al., 2014). Over the previous research on microfibers based DNA measurement, Leung et al. reported a method of detecting a model protein bovine serum albumin (BSA) using antibody-immobilization technique based on a tapered fiber-optic biosensor (Leung et al., 2007) and later studied the label-free detection of DNA hybridization using a gold-coated tapered fiber-optic biosensor (Leung et al., 2008). More recently, an idea of inscribing FBG into a microfiber named "microfiber Bragg grating (mFBG)" has been proposed and rapidly developed (Fang et al., 2010; Zhang et al., 2010; Chung et al., 2012; Kou et al., 2012), especially in the field of biomedical sensing (Chryssis et al., 2005; Saini et al., 2007; Shivananju et al., 2013). However, surface functionalization of the fiber sensor together with new interrogation method is still challenge for the detection of very slight amounts of bio-samples, down to a single molecule.

In this paper, a reflective fiber-optic biosensor with a compact mFBG configuration for specific DNA target sequences detection

* Corresponding author. Tel.: +86 20 85220665; fax: +86 20 85222046.
E-mail address: tguanbo@jnu.edu.cn (B.-O. Guan).

http://dx.doi.org/10.1016/j.bios.2014.05.065

in situ has been proposed and experimentally demonstrated. The mFBG provides two well-defined resonances in reflection, which show different sensitivities to RI and the same sensitivity to temperature. By monitoring the wavelength separation between these two resonance peaks, temperature-compensated RI measurement has been achieved. This device not only provides temperature-self-compensation ability but also has advantage of designable RI sensitivity by optimizing the diameter of microfiber. The surface of bare mFBG is functionalized with a monolayer of poly-L-lysine (PLL) and a single-stranded DNA probe (ssDNA), which works as high specificity biosensors for a given target ssDNA to form the double-stranded DNA (dsDNA) (Rindorf et al., 2006; Jang et al., 2009). The hybridization processes of the target ssDNA with the various concentrations have been monitored *in situ* with the lowest concentration of 0.5 μM. The detection process is precisely controlled with a micro-fluidic chip which allows the measurement of μL-volumes of bio-samples. The proposed mFBG-based biosensor is an appealing solution for rapid, sub-microliter dose and highly sensitive detection of analytes in medicine, chemical and environmental applications.

2. Reflective mFBG sensor

2.1. Fabrication of mFBG sensor

Here in this work, high-efficiency fabrication of mFBGs is accomplished by use of a 193 nm excimer laser and phase mask method. Here microfibers are drawn from a commercial multimode fiber (MMF) manufactured by Corning Inc. with core/cladding diameter of 62.5/125 μm. The microfibers are drawn and tapered by heating method using a butane flame brushing, with heating time about tens of seconds. This treatment not only is helpful for achieving low loss microfiber with good noise suppression, but also is capable to solve the degradation of microfibers due to the surface contamination during preservation (Brambilla et al., 2006). Meanwhile, flame brushing also contributes to the photosensitivity enhancement of microfibers (Bilodeau et al., 1993). Owing to the high efficiency associated with two-step absorption at 193 nm (Albert et al., 1995), the gratings can be directly inscribed in the microfibers with high efficiency, without hydrogen loading or other photosensitization treatment. Meanwhile, it should be note that, compared to microfiber draw from SMF, MMF based microfibers provide a much larger photosensitive region over microfiber cross section due to the larger Ge-doped region and lead to much higher grating inscription efficiency (Ran et al., 2012).

The mFBGs are manufactured using the phase-mask technique by using 193 nm ArF excimer laser. The phase mask is with a period of 1070.49 nm. The energy and repetition rate of the ArF excimer laser are set to 3 mJ/pulse and 200 Hz (corresponding to an average laser power of 0.6 W). The distance of the microfiber from the phase mask is about 100 μm. A cylindrical lens is used to focus the ArF excimer laser beam to an energy density of 120 mJ/cm^2 on the microfiber. The time for grating inscription over a microfiber (without hydrogen loading) is about 5 min.

Microfibers with diameters range from 3 to 10 μm have been shown in Fig. 1(a). Fig. 1(b) presents the reflection spectrum of mFBG with diameter of 3.9 μm, which is composed of two privileged modes (Ran et al., 2011). The 3 dB bandwidths of the fundamental mode (λa) and the high-order mode (λb) are 2.1 nm and 0.27 nm, respectively, with a wavelength separation of 22.5 nm. To gain a better understanding of the spectral characteristics of mFBG, we used numerical mode simulation (COMSOL) to analyze the composition of the two resonances in reflection and the transverse electric field amplitude distributions of their constituent modes, as shown in the bottom insets of Fig. 1. It is clear that the high-order mode has stronger evanescent field on microfiber surface than the fundamental mode.

2.2. Characterization of mFBG sensor

The sensing characteristics of bare mFBG to surrounding RI (1.33–1.44) and temperature (20–90 °C) changes have been shown in Fig. 2. In details, Fig. 2(a) and (b) presents that the fundamental mode (λa) and the high-order mode (λb) are with different sensitivities to surround RI fluctuations. In general, the thinner the microfiber is (here diameter range from 3 to 5 μm), the higher

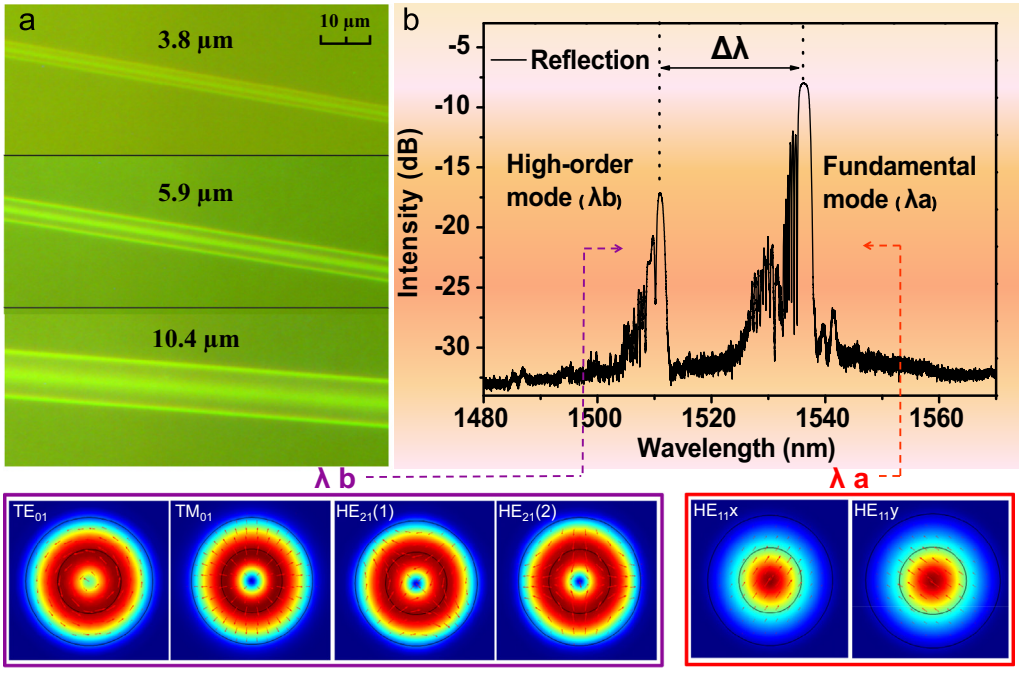

Fig. 1. (a) Microscope images of the tapered microfibers with different diameters; (b) the reflection spectrum of mFBG with diameter of 3.9 μm, insets show the composition of above two reflective resonances and the transverse electric field amplitude distributions of their constituent modes.

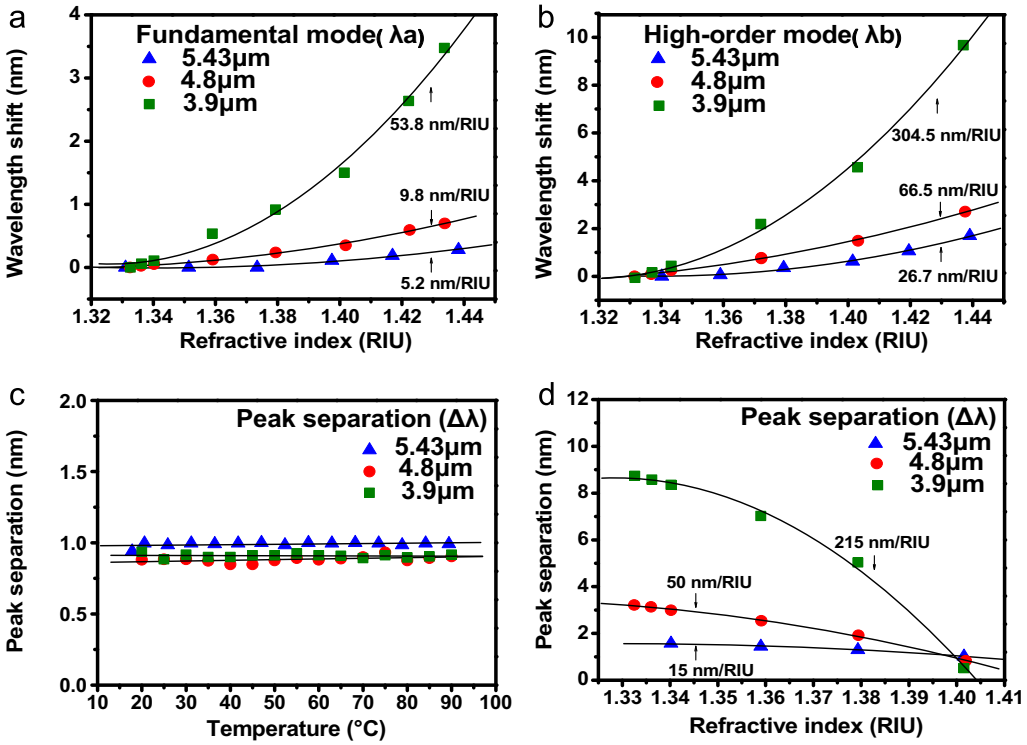

Fig. 2. Relationships between peak wavelength shift and RI of mFBGs with different diameters: (a) fundamental mode (λa) and (b) high-order mode (λb), wavelength separation ($\Delta\lambda=\lambda a-\lambda b$) response to (c) temperature fluctuations and (d) RI, respectively.

RI sensitivity can be achieved. However, it should be noted that there is a tradeoff between RI sensitivity and transmission loss (together with stability). Meanwhile, compare to the fundamental mode (Fig. 2(a)), the high-order mode (Fig. 2(b)) of mFBG provides a much higher RI sensitivity (304.5 nm/RIU for microfibers with diameter of 3.9 μm), because of its stronger evanescent field on the surface of the fiber sensor, as the transverse electric field amplitude distributions shown in Fig. 1.

Another important issue is to eliminate the temperature cross-sensitivity from RI measurement. Because both the fundamental mode and the high-order mode have the same thermal-expansion coefficient and thermo-optic coefficient (these two effects dominate the temperature sensitivity), resulting in that the two peaks have the same sensitivity to temperature, as the experimental results shown in Fig. 2(c). Therefore, the wavelength separation ($\Delta\lambda=\lambda a-\lambda b$) between the two peaks is free from temperature perturbations, as shown in Fig. 2(c), and so temperature-compensated RI measurement can be realized. Finally, Fig. 2(d) presents that the sensitivity of wavelength separation ($\Delta\lambda$) to surrounding RI can be increased with the decrease of the microfiber diameter. Our biosensor used in the following section is based on the mFBG with diameter around 4 μm. It has RI sensitivity of 215 nm/RIU.

3. Materials and methods

3.1. Surface functionalization of mFBG biosensor

Similar to previous works (Rindorf et al., 2006; Jang et al., 2009), because the surface of silica microfiber is inherently negative-charged (Hea et al., 2011), the surface functionalization of fiber sensor can be divided into the following two steps:

(a) Reaction of poly-L-lysine (PLL) with the positive charges of amino group (0.1% w/v in water, the molecular weight= 150,000–300,000 g/mol), process for 1 h.

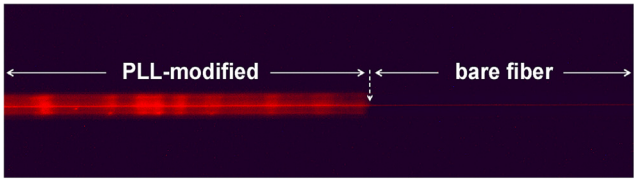

Fig. 3. Fluorescent image of the PLL-modified fiber (left) and the bare fiber (right) after infiltration of fluorescent-labeled DNA sequences.

(b) Reaction of probe ssDNA with negative charges, process for 1 h.

A monolayer of PLL with positive charges is immobilized onto the negatively charged fiber surface. Then probe ssDNA (5′ > TCC AGA CAT GAT AAG ATA CAT TGA TG < 3′) with negative-charged phosphate groups can be immobilized on the surface of PLL. Thus, DNA probe is ready for target DNA hybridization (target complementary ssDNA 5′ > CA TCA ATG TAT CTT ATC ATG TCT GGA < 3′). Meanwhile, the non-complementary ssDNA (5′ > CTCACGTTAATGCATTTTG-GTC < 3′) has also been tested to evaluate the specificity of the proposed sensor and its cross sensitivity. It should be noted that the probe ssDNA cannot be effectively bound onto the bare silica fiber (that is why a monolayer of PLL surface deposition is necessary). Fig. 3 gives a directly comparison about this point. Here a bare silica fiber with and without PLL-surface-modification is filled into fluorescent-labeled DNA solution, and the fluorescent image shown in Fig. 3 clearly identifies the difference (achieved by an inverted fluorescence microscopy with 543 nm laser source for the excitation of the Cy3 fluorophore).

Fig. 4 shows the scanning electron microscopy (SEM) images of a microfiber biosensor (inscribed with mFBG, Fig. 4(a)) and a commercial unshaped SMF (for comparison, Fig. 4(b)) after target DNA hybridization (with the same concentration of 1 μM). In contrast of a few sparse bio-particles binding over SMF, microfiber biosensor presents a much thicker and uniform bio-film over its surface. The improved adhesion capability of bio-particle contributes

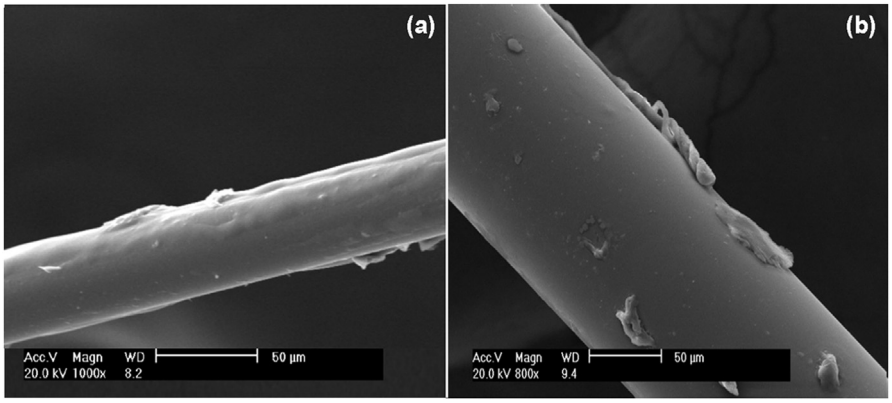

Fig. 4. Scanning electron microscopy (SEM) images after DNA hybridization: (a) tapered microfiber and (b) unshaped SMF.

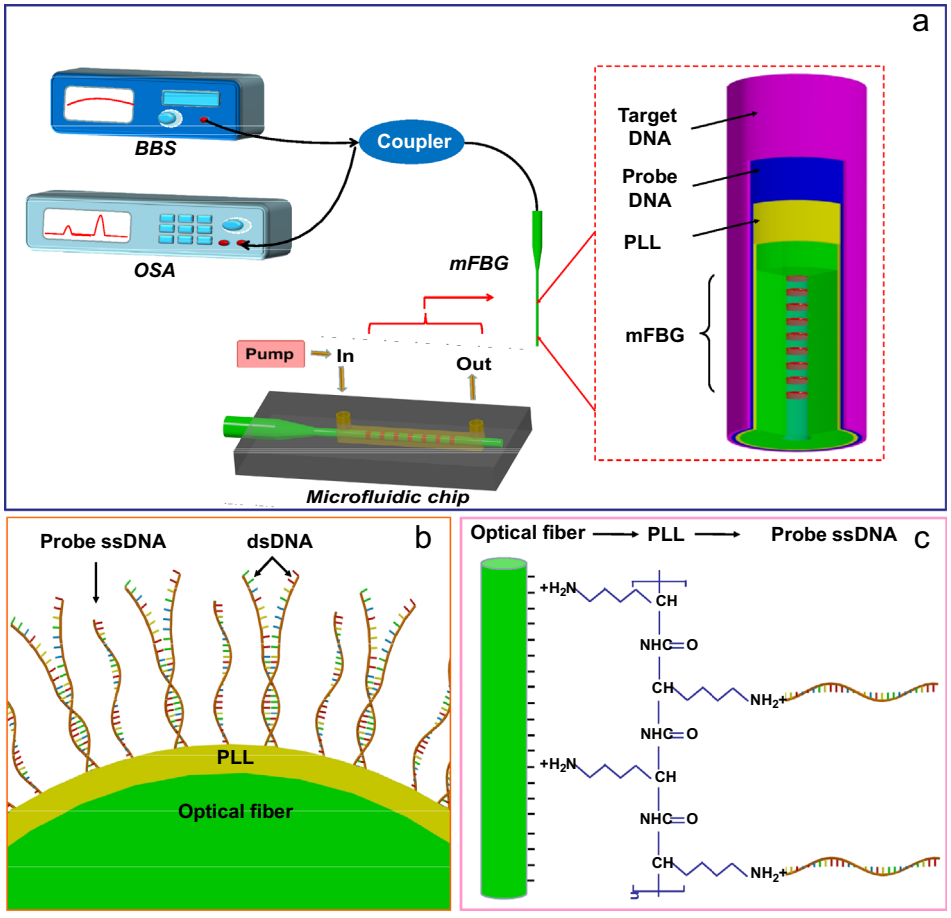

Fig. 5. (a) The schematic of the optical setup of mFBG biosensor (inset zooms in the configuration of the sensor probe and the micro-fluidic chip), (b) the scheme of surface functionalization of mFBG biosensor, and (c) the sandwich-like probe system used for target DNA detection.

significantly to an improved sensitivity for analytes detection of at low concentrations.

3.2. Experimental setup and optical configuration

The experimental setup permits the sensor to operate in the reflection, as the schematic of the optical setup shown in Fig. 5(a). The scheme of surface functionalization of mFBG biosensor is presented in Fig. 5(b), together with the sandwich-like probe system used for target DNA detection, as shown in Fig. 5(c). During the experiments, the sensor probes are fixed in PDMS (polydimethylsiloxane)-based micro-fluidic channels designed specifically for the biosensing tests. While each individual sensor is fixed in the micro-channel (width 200 µm by height 150 µm) with help of UV-sensitive adhesive both sides over the sensing element of 2–3 cm in length (for a total sensing volume of ~50 µL, taking into account the volume taken up by the fiber). Biosample solutions are injected into the micro-fluidic chip (Fig. 5(a)) via an electronic-controlled pump, eliminating the potential environmental influence during the bio-sample measurement. The sensing mFBG is excited by a broadband source (BBS) with light over the 1250–1650 nm range and its reflection spectrum is monitored

by an optical spectrum analyzer (OSA) with minimum wavelength resolution of 0.02 nm. The measurements are recorded continuously at a rate of one spectrum every 30 s.

4. Results and discussion

Fig. 6 presents the real-time peak-wavelength-separation ($\Delta\lambda$) response of three surface-functionalized mFBG biosensors fabricated on microfibers with slightly different diameters around 4 μm over repeated testing procedures (I: PLL deposition, II: probe DNA binding, and III: DNA hybridization) for target DNA detection with different concentrations (DNA@1 μM, DNA@0.5 μM, DNA@0.1 μM) respectively. For the procedure I, the deposition of a monolayer PLL (RI = 1.3334) induces a negligible wavelength shift because its RI is quite similar to that of buffer solution (saline). For the procedure II, the PLL-modified mFBG biosensors are immersed in the probe ssDNA solution (RI = 1.3725) with concentration of 20 μM (i.e. nmol/mL). Due to the probe ssDNA binding over time, the RI of fiber surface will be gradually increased. This will induce a strong red-shift of high-order mode (λb) but little to the fundamental mode (λa), because of their different transverse electric field amplitude distributions (as shown in Fig. 1) and surround RI sensitivity (as shown in Fig. 2). Therefore, the wavelength separation ($\Delta\lambda$) will be gradually decreased. After procedure I and II, the mFBG biosensor is ready for target DNA hybridization. Meanwhile, it should be explained that, over the procedure I and II, the three response curves (corresponding to probe 1 of mFBG@4.2 μm, probe 2 of mFBG@3.9 μm, probe 3 of mFBG@4.0 μm) show slight differences. This is because it is hard for us to fabricate microfibers with exactly same diameter at present (further works will be carried out to improve the drawing technique). Procedure III demonstrates that target DNA hybridization information can be *in-situ* obtained for low DNA concentrations of 1 μM and 0.5 μM, respectively. While for the DNA concentration lower than 0.5 μM (as the results of 0.1 μM shown in Fig. 6), the proposed sensor comes to its limit of detection. Meanwhile, experimental results show that there is no spectral change when the sensor is immersed into the non-complementary of DNA solution (DNA sequences see Section 3.1), which identifies the specificity of the proposed sensor.

The repeatability of proposed sensor can be confirmed if the peak wavelength of two resonances in reflection can remove back to their original positions over repeat measurement (process III). We used the recovery method reported early (Chen et al., 2007), that is immersing the used biosensor (after DNA hybridization) with a freshly prepared buffer of 5 mM Na_2HPO_4 and 0.1% (w/v) sodium dodecyl sulfate (SDS) at 95 °C for 3 × 30 s. Fig. 7 presents the real-time response of mFBG sensors for 3 times repeat target DNA hybridization (process III). The results show that the surface functionalization of mFBGs can be reused but still face the problem of non-negligible memory effect (the original peak separation cannot recover totally). The insets of Fig. 7 present the average outputs and errors for 3 times repeat DNA hybridization processes, which further identify that the lowest detectable concentration of the mFBGs sensor is estimated to be 0.5 μM.

5. Conclusion

We proposed a compact biosensor based on a surface-functionalized mFBG for specific DNA sequences detection. By monitoring the wavelength separation of two well-defined resonances of mFBG in reflection, high sensitivity RI measurement has be achieved together with eliminated the temperature cross-sensitivity. The label-free bio-recognition scheme is achieved by surface functionalization of the bare mFBG with a monolayer of PLL and synthetic probe ssDNA sequences. The hybridization processes of the target ssDNA with the various concentrations have been monitored *in situ* with the lowest concentration of 0.5 μM. Combined with micro-fluidic technology, the detection process can be precisely controlled with as little as μL-volumes of

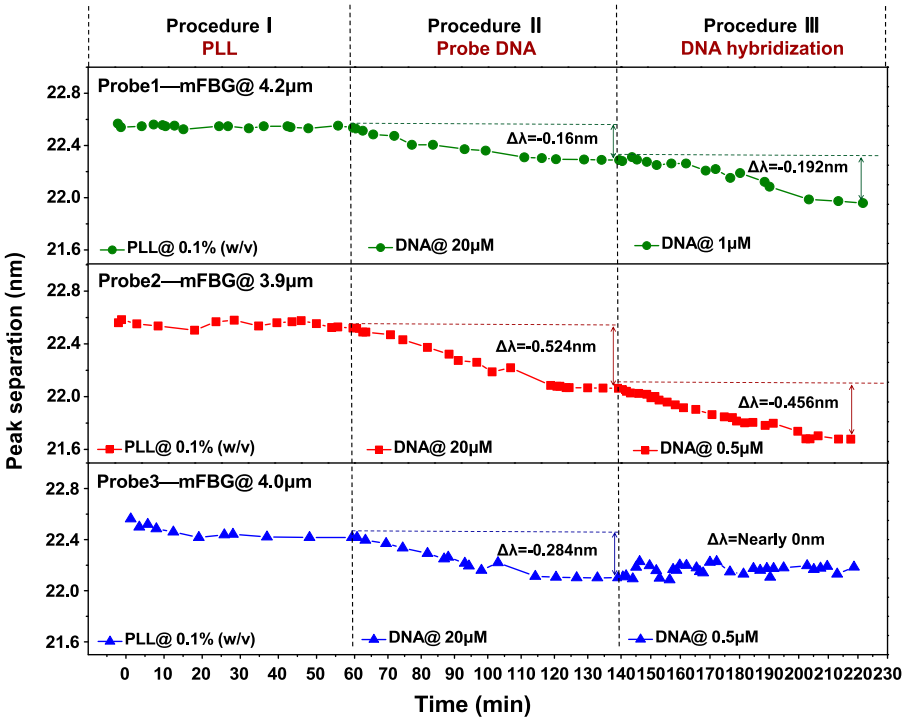

Fig. 6. Real-time peak separation ($\Delta\lambda$) response of the surface-functionalized mFBG-biosensors versus PLL deposition, probe DNA binding and DNA hybridization.

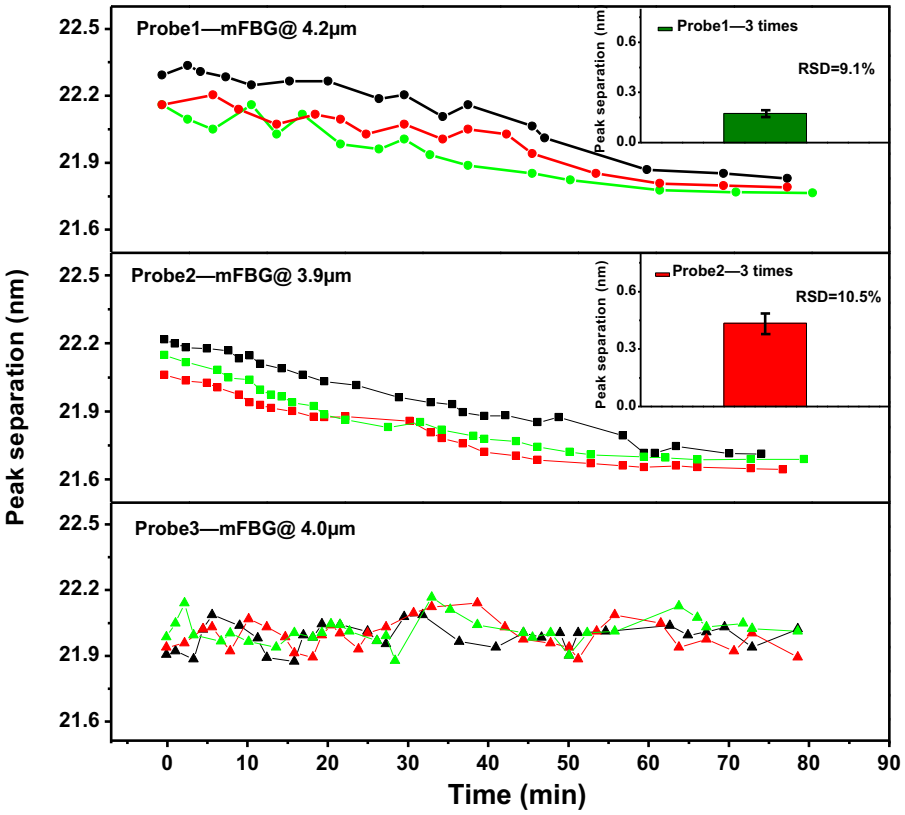

Fig. 7. Real-time peak separation ($\Delta\lambda$) response of the surface-functionalized mFBG-biosensors for repeat DNA hybridization. Insets show the output averages and errors.

bio-samples. The sensor itself is very easy to manufacture at very low cost and to interrogate using standard telecommunications-based instrumentation. Therefore, it is a good candidate for rapid and highly sensitive detection in microliter volumes of analytes at low concentrations (0.5 μM) in medicine, chemical and environmental monitoring.

Acknowledgment

This work was supported by the National Science Fund for Distinguished Young Scholars of China (No. 61225023), the Research Fund for the Doctoral Program of Higher Education (Nos. 20114401110006, 20114401120006), the Pearl River Scholar for Young Scientist (No. 2011J2200014), the Planned Science and Technology Project of Guangzhou (No. 2012J5100028), and the Guangdong Natural Science Foundation (S2013030013302).

References

Albert, J., Malo, B., Hill, K.O., Bilodeau, F., Johnson, D.C., Theriault, S., 1995. Appl. Phys. Lett. 67, 3529–3531.
Bilodeau, F., Malo, B., Albert, J., Johnson, D.C., Hill, K.O., Hibino, Y., Abe, M., Kawachi, M., 1993. Opt. Lett. 18, 953–955.
Brambilla, G., Xu, F., Feng, X., 2006. Electron. Lett. 42, 517–518.
Candiani, A., Bertucci, A., Giannetti, S., Konstantaki, M., Manicardi, A., Pissadakis, S., Cucinotta, A., Corradini, R., Selleri, S., 2013. J. Biomed. Opt. 18, 057004.
Chen, X.F., Zhang, L., Zhou, K.M., Davies, E., Sugden, K., Bennion, I., Hughes, M., Hine, A., 2007. Opt. Lett. 32, 2541–2543.
Chryssis, A.N., Saini, S.S., Lee, S.M., 2005. IEEE J. Sel. Top. Quant. Electron. 11, 864–872.
Chung, K.M., Liu, Z., Lu, C., Tam, H.Y., 2012. IEEE Photon. J. 4, 437–442.
Corres, J.M., Matias, I.R., Bravo, J., Arregui, F.J., 2008. Sens. Actuators B: Chem. 135, 166–171.
Delport, F., Pollet, Janssen, J., K., Verbruggen, B., Knez, K., Spasic, D., Lammertyn, J., 2012. Nanotechnology 23, 065503.
Fan, X.D., White, I.M., Shopova, S.I., 2008. Anal. Bioanal. Chem. 620, 8–26.
Fang, X., Liao, C.R., Wang, D.N., 2010. Opt. Lett. 35, 1007–1009.
Guo, T., Liu, F., Liu, Y., Chen, N.K., Guan, B.O., Albert, J., 2014. Biosens. Bioelectron. 55, 452–458.
Hea, Z.H., Tian, F., Zhu, Y., Lavlinskaia, N., Du, H., 2011. Biosens. Bioelectron. 26, 4774–4778.
Jang, H.S., Park, K.N., Kim, J.P., Sim, S.J., 2009. Opt. Express 17, 3855–3860.
Kou, J.L., Ding, M., Feng, J., Lu, Y.Q., Xu, F., Brambilla, G., 2012. Sensors 12, 8861–8876.
Latifi, H., Zibaii, M.I., Hosseini, S.M., Jorge, P., 2012. Photonic Sens. 2, 340–356.
Leung, A., Shankar, P.M., Mutharasan, R., 2008. Sens. Actuators B: Chem. 131, 640–645.
Leung, A., Shankar, P.M., Mutharasan, R., 2007. Sens. Actuators B: Chem. 123, 888–895.
Li, K.W., Liu, G.G., Wu, Y.H., Hao, P., Zhou, W.C., Zhang, Z.Q., 2014. Talanta 120, 419–424.
Long, F., He, M., Shi, H.C., Zhu, A.N., 2008. Biosens. Bioelectron. 23, 952–958.
Nguyen, L.V., Warren-Smith, S.C., Cooper, A., Monro, T.M., 2012. Opt. Express 20, 29378–29385.
Ran, Y., Jin, L., Tan, Y.N., Sun, L.P., Li, J., Guan, B.O., 2012. IEEE Photonics J. 4, 181–186.
Ran, Y., Tan, Y.N., Jin, L., Sun, L.P., Gao, S., Li, J., Guan, B.O., 2011. Opt. Express 19, 18577–18583.
Rindorf, L., Jensen, J.B., Dufva, M., 2006. Opt. Express 14, 8224–8231.
Saini, S.S., Stanford, C., Lee, S.M., Park, J., DeShong, P., Bentley, W.E., Dagenais, M., 2007. IEEE Photonics Technol. Lett. 19, 1341–1343.
Shivananju, B.N., Renilkumar, M., Prashanth, G.R., Asokan, S., Varma, M.M., 2013. J. Lightwave Technol. 31, 2441–2447.
Tian, Y., Wang, W.H., Wu, N., Zou, X.T., Wang, X.W., 2011. Sensors 11, 3780–3790.
Tong, L.M., Gattass, R.R., Ashcom, J.B., He, S., Lou, J.Y., Shen, M., Maxwell, I., Mazur, E., 2003. Nature 426, 816–819.
Tripathi, S.M., Bock, W.J., Mikulica, P., Chinnappan, R., Ngb, A., Tolba, M., Zourob, M., 2012. Biosens. Bioelectron. 35, 308–312.
Voisin, V., Pilate, J., Damman, P., Mégret, P., Caucheteur, C., 2014. Biosens. Bioelectron. 51, 249–254.
Wang, X.W., Cooper, K.L., Wang, A., Xu, J.C., Wang, Z., Zhang, Y., Tu, Z.J., 2006. Appl. Phys. Lett. 89, 163901.
Yin, M.J., Wu, C., Shao, L.Y., Chan, W.K.E., Zhang, A.P., Lu, C., Tam, H.Y., 2013. Analyst 138, 1988–1994.
Zhang, Y., Lin, B., Tjin, S.C., Zhang, H., Wang, G.H., Shum, P., Zhang, X.L., 2010. Opt. Express 18, 26345–26350.
Zibaiia, M.I., Kazemi, A., Latifi, H., Azar, M.K., Hosseini, S.M., Ghezelaiagh, M.H., 2010. J. Photochem. Photobiol. B 101, 313–320.